Polarisation of Light

PHYS3114 - Electrodynamics

Toby Nguyen - z5416116

Contents

1 Revised Plots

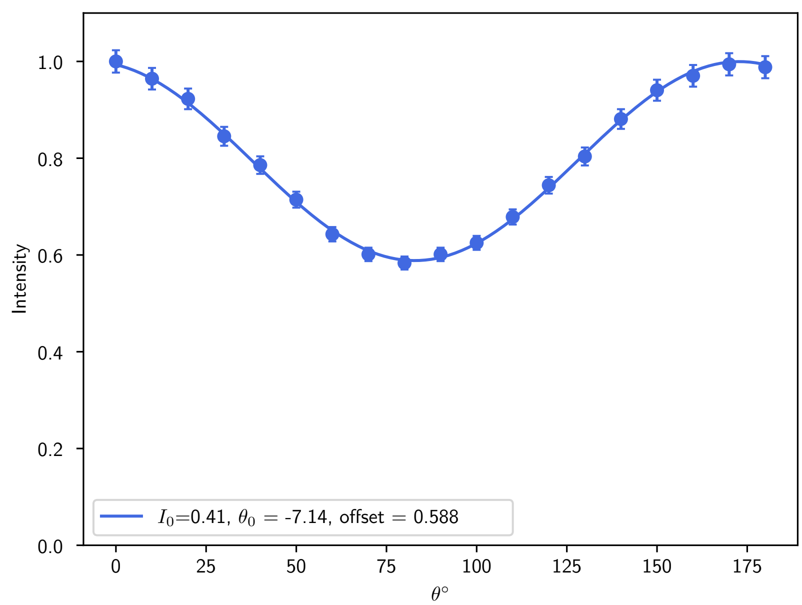

Figure 1: Normalised plot of intensity versus angle for a quarter wave plate. The intensity is bound within 20% of the mean which displays less angular dependence than no quarter wave plate but still some dependence nonetheless.

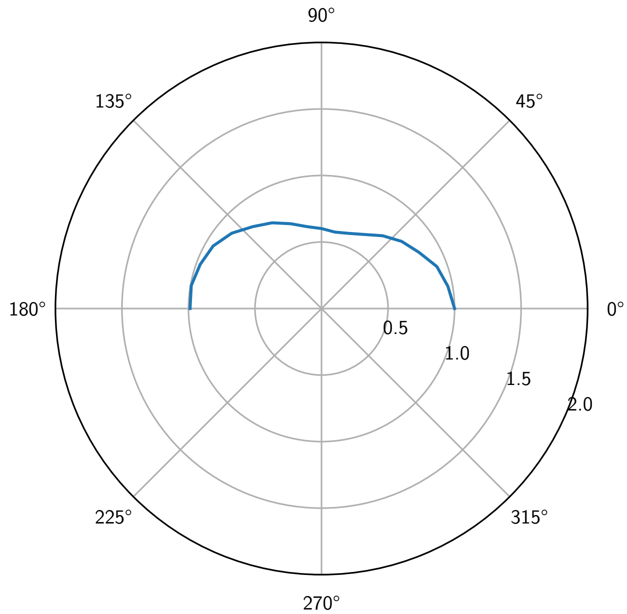

Figure 2: Polar plot of the intensity versus angle for the quarter wave plate. We notice it is jagged and not following clear curvature, potentially indicating high random error in the data collected.

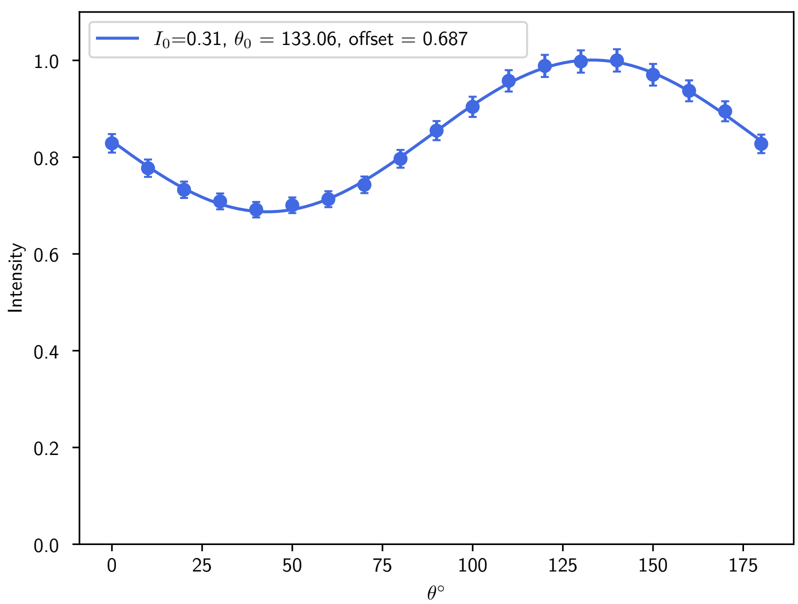

Figure 3: Normalised plot of intensity versus angle for the circular wave plate. We should expect the intensity to be independent of the angle measured however experimentally we find that is not the case.

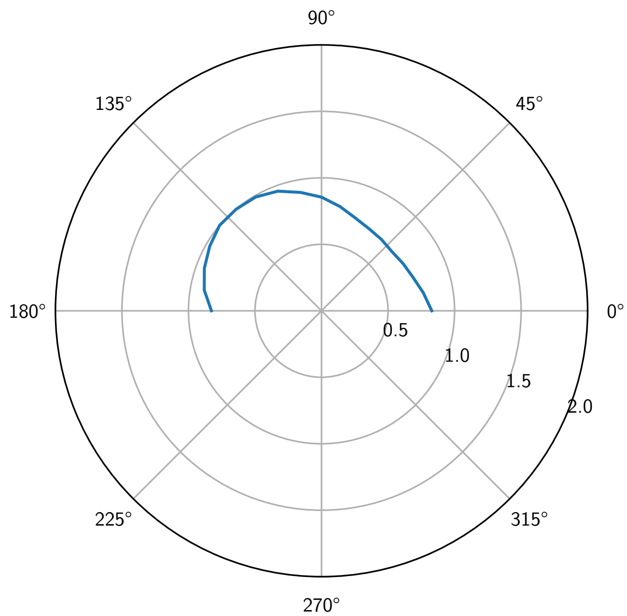

Figure 4: Polar plot of the intensity versus angle for the circular wave plate. We expected the polar plot to show a perfect top half of a semi-circle.

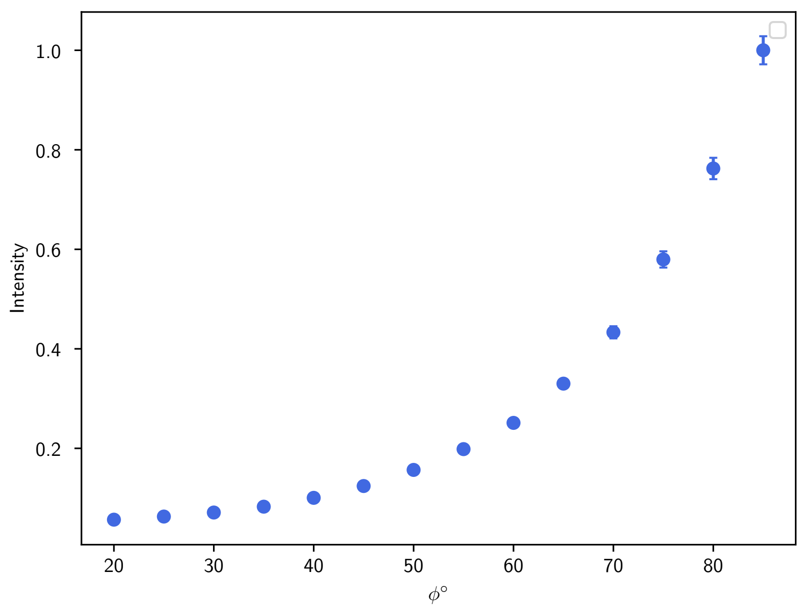

Figure 5: Fresnel equation experiment for vertically polarised light. It is monotonically increasing as for light parallel to the plane of incidence, it is unaffected by the polarisation due to reflection from the dielectric.

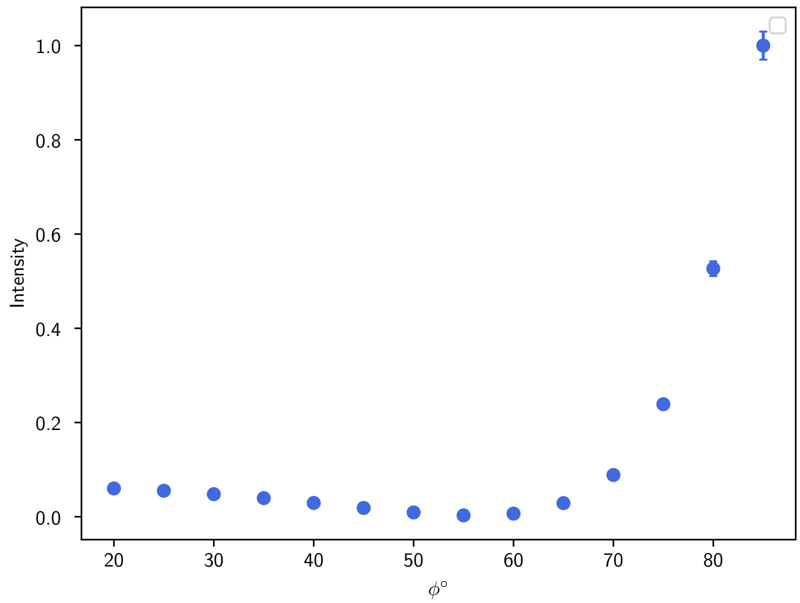

Figure 6: Unlike vertical polarised light, horizontally polarised light is perpendicular to the plane of incidence and so will be affected by the polarisation due to reflection on the dielectric material. The polarisation will increase up until Brewster's angle when the incident light is maximally polarised. Any angle past Brewster's angle, the polarisation reverses but begins to decrease.

2 Introduction

In this report we will explore the wave nature of light through the lens of polarisation. Polarisation played a pivotal role in the development of our understanding of light. With the polarising debate between Huygens and Newtons' differing theories of the model of light, few features of light distinguished the two competing theories such as interference, polarisation and diffraction.

Focusing in on polarisation, we want to first investigate the interaction of an photon scattered on a molecule. Initially, quantified by Lord Rayleigh, we find that the intensity of scattering is dependent on the wavelength of the incoming light, given that the linear dimensions of the particles are much smaller than the wavelength. This mechanism is driven by the notion that when the reflector is much smaller than the wavelength, the spreading is so great that the reflected waves differ very little from uniform spherical waves, i.e little interaction between reflected light, so the law of reflection ceases to be applicable. However as the wavelength becomes comparable in size with the molecule, we have Mie scattering which will scatter light independent of its wavelength so it produces more opaqueness or cloudiness. The Mie scattering effect will increase with particle size.

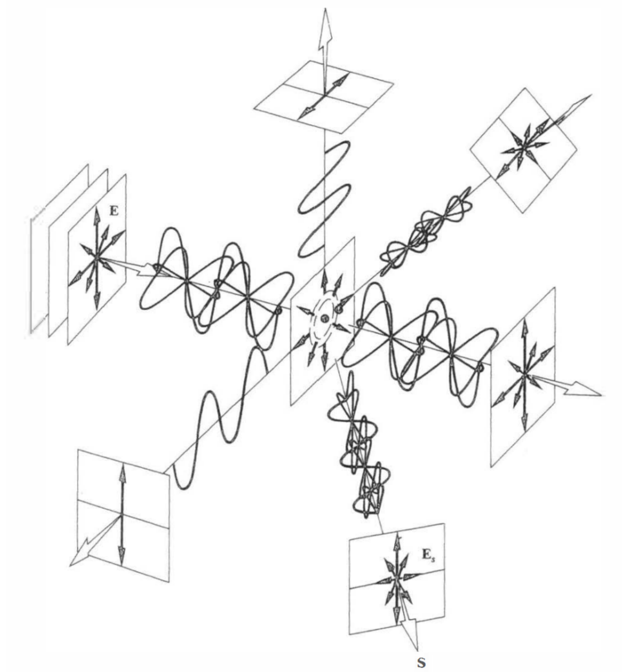

Figure 7: Diagram showing unpolarised light incident on a molecule much smaller than the wavelength of the light. Note the polarising effect of scattering dependent on the angle of observation. This is due to the electric dipole oscillation patterns.

When photons excite electrons such as in the case of scattering above, there will be energy released in the form of electric dipole radiation. The excitation of electrons will produce an oscillation of the dipole in the molecule. The electric field lines of these oscillations are shown in Figure 8 below.

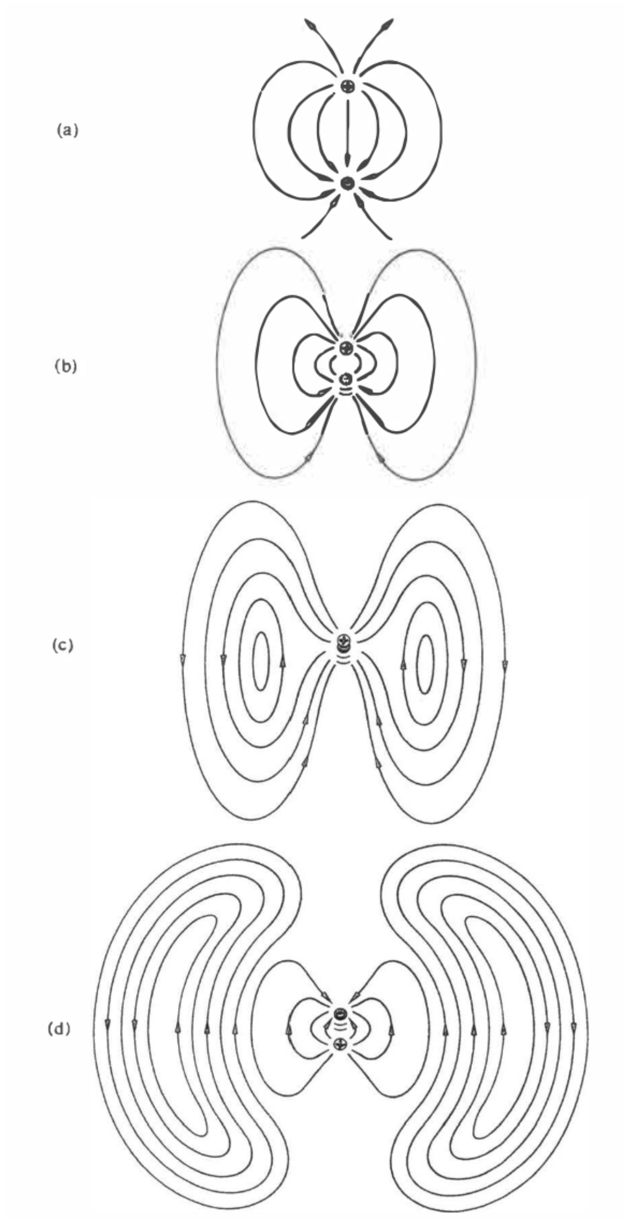

Figure 8: Electric field lines of oscillating dipoles. Note the lack of electric field in the direction parallel to the direction of oscillation.

Moving away from scattering, we can further analyse the nature of polarisation through investigating Malus' Law. This law states that the transmitted intensity varies as the square of the cosine of the angle between two planes of transmission,

$$I = I_0 \cos^2 \theta. \tag{1}$$

Birefringent materials are anisotropic, meaning their polarisability will depend on the orientation of light coming through. These materials have two axes, fast and slow, which possess different refractive indices. This means that there will be a phase delay between the two refracted beams of light whereby,

$$\Delta\phi = \frac{2\pi}{\lambda}(n_e - n_o)d. \tag{2}$$

If the phase delay is π, then this will lead to a rotation of linear polarisation. Quarter-wave plates have phase delays corresponding to $\frac{\pi}{2}$. Circular polarisation of light can be done by taking linearly polarised light and transmitted it through a quarter wave plate.

The phenomenon of polarising light can also be found when light is reflected by dielectrics materials.

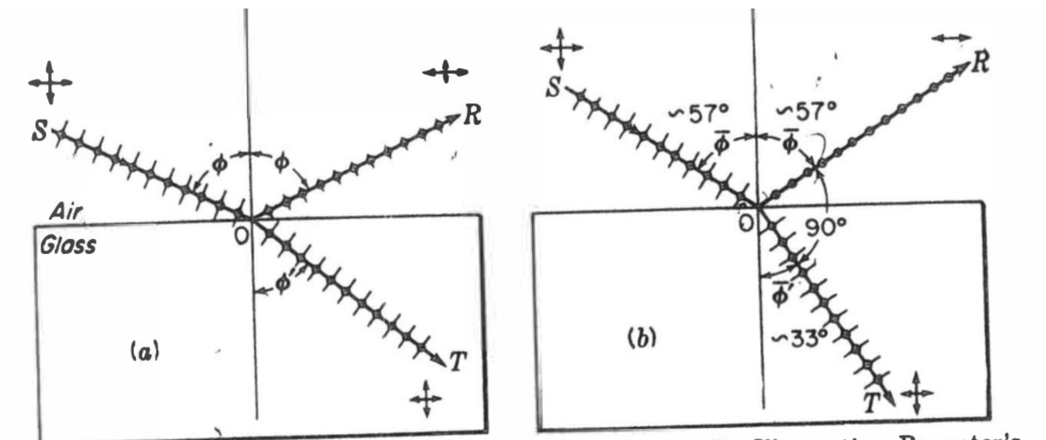

FIG. 24D. (a) Polarization by reflection and refraction. (b) Illustrating Brewster's law for the polarizing angle.

Figure 9: Diagram showing a special angle where the reflected beam of light becomes fully polarised in one direction. This is because of the direction of the electric dipole radiation mentioned before, now it is the reradiation that generates the reflected beam and so only polarised light orthogonal to the plane of incidence will be produced.

Using Snell's law, we can derive the equation for Brewster's angle for incident light coming from air,

$$\tan\theta_B = n. \tag{3}$$

At different angles, the reflected light is only partially polarised and so arises two orthogonal components of the light, one parallel to the plane of incidence, subscripted p and one perpendicular to the plane of incidence, subscripted s. The reflectance coefficients describes the percentage of light reflected and can be decomposed into these two different alignments. Derived by Fresnel, his laws of reflection states that,

$$\frac{R_s}{E_s} = \frac{\sin(\theta - \theta')}{\sin(\theta + \theta')}, \tag{4}$$

and

$$\frac{R_p}{E_p} = \frac{\tan(\theta - \theta')}{\tan(\theta + \theta')}. \tag{5}$$

When the light hits the dielectric material at the normal incidence, we can say that θ and θ' become small and so we can equate the sines to the tangents, combining our two reflectance equations into one simple and elegant result,

$$r = \frac{R^2}{E^2} = \frac{(1-n)^2}{(1+n)^2}. \tag{6}$$

In the case of metals which have a complex refractive index with a imaginary coefficient k to denote the absorption strength of the material, we have the generalised equation,

$$R = \frac{(1-n)^2 + k^2}{(1+n^2) + k^2}. \tag{7}$$

Different angles of incidence will also influence the direction of polarisation of the reflected beam, hence the existence of the Brewster's angle. As Brewster's angle represents the point at which the light is maximally polarised, this must lead to it being the point at which the polarisation direction of the parallel component switches.

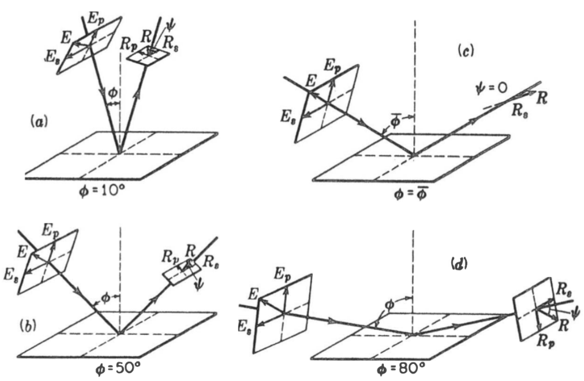

Figure 10: Light incident on a dielectric will produce a polarised reflected beam whose polarisation is dependent on the angle of incidence compared to the Brewster's angle.

Finally, light incident on a metal will be partially absorbed and reflected, depending on the refractive index of the metal. Aforementioned, there exists a k term to represent the metal's absorption strength and so the phase delay upon reflection is also dependent on the finite peneration depth of light into the material, given by,

$$\Delta\phi = \tan^{-1}\left(\frac{2k}{1-n^2-k^2}\right). \tag{8}$$

3 Jones vectors

Throughout the report, we will be using Jones vectors and matrices to represent the tranmission of light. Jones vectors are representations of a polarisation state, generally denoted as,

$$\mathbf{J} = \begin{pmatrix} E_{0x} \\ E_{0y} \end{pmatrix}. \tag{9}$$

[1]

[1]Phase changes will be omitted as we will only be using Jones notation to derive relationships for intensity of light.

Once we have a polarisation state, we can apply polarisers on it, represented by Jones matrices. The action of a polariser angled at θ on an input polarisation state is given by,

$$\mathbf{J'} = R(-\theta)PR(\theta)\mathbf{J}, \tag{10}$$

where R is the rotation matrix and P is the polariser used.

The intensity of light can then be found by taking the magnitude or norm of the vector $\mathbf{J'}$.

4 Experimental Setup and Error Analysis

The most basic setup is shown in Figure 11 below.

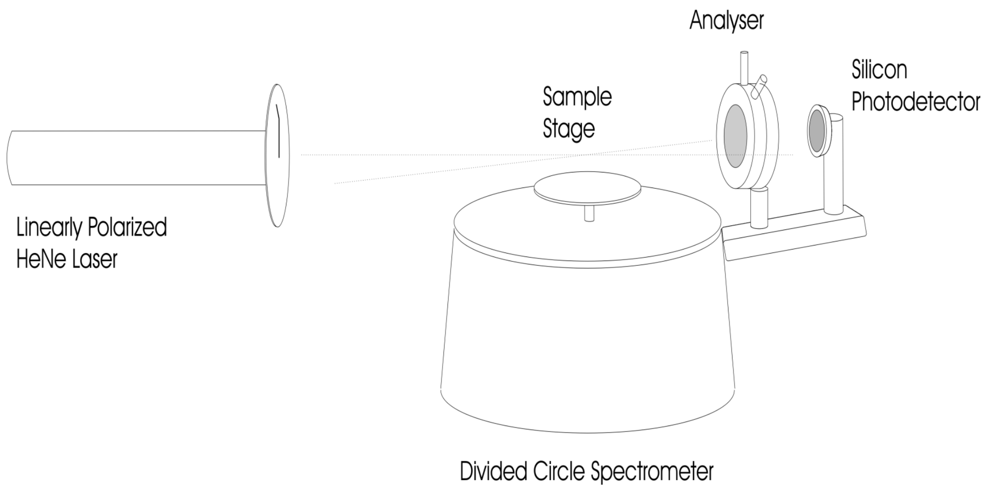

Figure 11: Schematic drawing of a basic experimental layout. Note that the spectrometer posseses two measurements, one for the orientation of the Vernier table, i.e the direction of the sample stage with respect to the laser and the second being the spectrometer arm in relation to the sample stage. The analyser and photodetector are also initially aligned with the laser in parallel.

The main driver of systematic error in this experiment was the maximum precision in measuring angles. There were four different angle measurements, one for the polariser in front of the laser, which had increments of 1 degree thus an absolute error of $\pm 0.5°$. This was the same for the analyser in front of the photodiode. The spectrometer came in increments of $\frac{1}{3}^{\circ}$, indicating an absolute error of $\pm\frac{1}{6}^{\circ}$ however due to wear and visibility, the absolute error was adjust to be $\pm 0.25°$. The spectrometer was used to measure the orientation of the Vernier table as well as the spectrometer arm. The uncertainty in the laser and the photodetector was taken to be negligible. The next major source of systematic error would be the misalignment of the components in the experiment. This would lead to unintended reflected beams from various components which would potentially alter the intensity reading by the photodetector. We quantified this error to be 1%. The error analysis for each experiment can be found in the Python code below.

```
#Error analysis

#Error for Experiment 1
#Sources of Error: Alignment of setup (1%) + Reading of halfwave plate (+- 0.5 / 199) +
                                            Reading of Spectrometer arm (+-0.25/90) +
                                            Analyser readings from 0 to 180
```

```
x0 = np.linspace(10,180,18)
analyser_error_exp1 = [0.5/i for i in x0]
rms_analyser_exp1 = np.sqrt(np.mean(np.square(analyser_error_exp1)))

exp1_err = np.sqrt(0.01**2+(0.5/199)**2+(0.25/90)**2+rms_analyser_exp1**2)

#Error for Experiment 2
#Sources of Error: Alignment of setup (1%) + Reading of halfwave plate (+- 0.5/199) +
                                              Analyser readings from 0 to 90

x1 = np.linspace(10,90,9)
analyser_error_exp2n3 = [0.5/i for i in x1]
rms_analyser_exp2n3 = np.sqrt(np.mean(np.square(analyser_error_exp2n3)))

exp2n3_err = np.sqrt(0.01**2 + (0.5/199)**2+rms_analyser_exp2n3**2)

#Error for Experiment 4a
#Sources of Error: Alignment of setup (1%) + Table reading (0.25/330) + Table reading 2 (0.
                                              25/21) + half wave plate reading (0.5/334)

exp4brewsters_err = np.sqrt(0.01**2+(0.25/330)**2+(0.25/21)**2+(0.5/334)**2)

#Error for Experiment 4b
#Sources for Error: Table reading (0.25/21.66) + Intensity (0.05/75.4) + Background reading
                                              (0.05/7.9) + Table reading 2 (0.25/226) + Arm
                                              (0.25/306) + Table rotation from 0 to 30
                                              degrees

x2 = np.linspace(5,30,6)
table_error_exp4 = [0.25/i for i in x2]
rms_table_exp4 = np.sqrt(np.mean(np.square(table_error_exp4)))

exp4bv_error = np.sqrt((0.25/21.66)**2+(0.05/75.4)**2+(0.05/7.9)**2+(0.25/226)**2+(0.25/306)
                                              **2+rms_table_exp4**2)
exp4bh_error = np.sqrt((0.25/21.66)**2+(0.05/55.3)**2+(0.05/4.4)**2+(0.25/227)**2+(0.25/306)
                                              **2+rms_table_exp4**2)

#Error for Experiment 4c
#Sources of Error: Alignment of setup (1%) + Table reading error (+-0.25/20) + Halfwave
                                              plate (0.5/221.5) + 1 Analyser Reading (0.5/
                                              312) or (0.5/236)
exp4_20_error = np.sqrt(0.01**2+(0.25/20)**2+(0.5/221.5)**2+(0.5/312)**2)
exp4_80_error = np.sqrt(0.01**2+(0.25/20)**2+(0.5/221.5)**2+(0.5/236)**2)

#Error for Experiment 5
#Sources of error: Waveplate reading (0.5/221.5) + Analyser reading (0.5/235) or (0.5/315) +
                                               Table reading (0.5/22.66) or (0.5/14)
exp5_20_error = np.sqrt((0.5/221.5)**2+(0.5/235)**2+(0.5/22.6)**2+rms_analyser_exp1**2)
exp5_79_error = np.sqrt((0.5/221.5)**2+(0.5/315)**2+(0.5/14)**2+rms_analyser_exp1**2)
```

As seen above, to account for multiple angle measurement uncertainties, the root mean squared was used rather than the mean. This is because higher uncertainty percentages, i.e smaller angles should be weighted greater.

5 Part I

5.1 Method

5.1.1 Scattering

In this half of the report, the setup shown in Figure 11 was used. We wanted to first investigate the polarisation pattern found in Figure 7. To do so, a container of Dettol solution was placed onto the sample stage with a vertically polarised laser pointing directly into its centre, illuminating the inside and scattering red light spherically from the container. The analyser was then rotated to give a maximum intensity reading and the spectrometer arm was rotated from $0°$ to $90°$ with respect to the beam. We should expect the intensity to remain constant because the incident light will excite the molecules to oscillate in the vertical direction, maximally polarising light vertically. This was then repeated for a horizontally polarised laser and now we should expect intensity to decrease as we approach the perpendicular observation direction.

We want to investigate the relationship between the spatial dimensions of the scattering medium and the intensity of the scattering. For this, we will compare the intensity of light perpendicular to the beam as it passes through a solution. As we are measuring the intensity from the perpendicular observation point, the orientation of the polarised laser must be in the vertical direction. We compare two solutions, Ajax and Dettol. By eye, Dettol is a much more cloudy and opaque liquid, indicating larger molecules as well as a greater number of molecules. We expect the intensity of scattering then to be greater for the Ajax solution as the size of the molecules will be finer, allowing for a higher fraction of independent scattered spherical waves sourced from each incident interaction of laser to molecule.

Next, we will explore Malus' law.

5.1.2 Polarisation

The initial polarisation on the laser is vertically orientated so we can represent this using the Jones vector,

$$\mathbf{y} = \begin{pmatrix} 0 \\ 1 \end{pmatrix}. \tag{11}$$

Or more specifically,

$$\mathbf{J} = \begin{pmatrix} 0 \\ E_{oy} \end{pmatrix}. \tag{12}$$

To find the Jones' matrix representation of an analyser at some angle θ to the plane of polarisation of the incoming light, we first consider some arbitrary reference frame for which the polariser is aligned with, at an angle θ. So we have to introduce a rotation matrix with angle θ to transform the coordinates into the reference frame of the polariser,

$$R_{+} = \begin{pmatrix} \cos\theta & \sin\theta \\ -\sin\theta & \cos\theta \end{pmatrix}. \tag{13}$$

We can now just apply the follow Jones matrix to remove any orthogonal components,

$$P_y = \begin{pmatrix} 0 & 0 \\ 0 & 1 \end{pmatrix}. \tag{14}$$

Now we can transform the coordinates back into the reference frame of the lab by applying the rotation matrix again but with $-\theta$,

$$R_- = \begin{pmatrix} \cos -\theta & -\sin\theta \\ \sin\theta & \cos\theta \end{pmatrix}. \tag{15}$$

Putting all of this together,

$$\mathbf{J'} = R_- P_y R_+ \mathbf{J}. \tag{16}$$

Computing the matrix multiplication will result in,

$$\mathbf{J'} = \begin{pmatrix} \sin^2\theta & -\cos\theta\sin\theta \\ -\cos\theta\sin\theta & \cos^2\theta \end{pmatrix} \mathbf{J}. \tag{17}$$

Substituting in Equation 12, we find,

$$\begin{aligned} \mathbf{J'} &= \begin{pmatrix} \sin^2\theta & -\cos\theta\sin\theta \\ -\cos\theta\sin\theta & \cos^2\theta^2 \end{pmatrix} \begin{pmatrix} 0 \\ E_{0y} \end{pmatrix} && (18) \\ &= E_{0y} \begin{pmatrix} \cos\theta\sin\theta \\ \cos^2\theta \end{pmatrix} && (19) \end{aligned}$$

Taking the magnitude of the Jones vector to represent its magnitude,

$$I = |\mathbf{J'}|^2 = E_{0y}(\sin^2\theta\cos^2\theta + \cos^4\theta). \tag{20}$$

Simplifying the equation and then replacing E_{0y} with I_0,

$$\begin{aligned} I &= I_0(\cos^2\theta(1-\cos^2\theta) + \cos^4\theta) && (21) \\ &= I_0\cos^2\theta. && (22) \end{aligned}$$

A result that is a little too long to display here but will be referenced in the appendix, in Appendix 7.3.1, is the fact that quarter wave polarisers will not affect the amplitude of the incoming wave, instead only introduce a phase delay. This means that we expect Malus's law to hold even for circularly polarised light, except with a phase delay.

Experimentally, to test the polarisation of light by analyser angles, quarter wave plates and circular polarisers, we can just use the same setup as found in Figure 11 with the filter or no filter on the sample stage. The intensity versus angle plot can be created by rotating the analyser through 180 degrees to see any periodic changes in the intensity of the transmitted light.

5.2 Results

5.2.1 Scattering

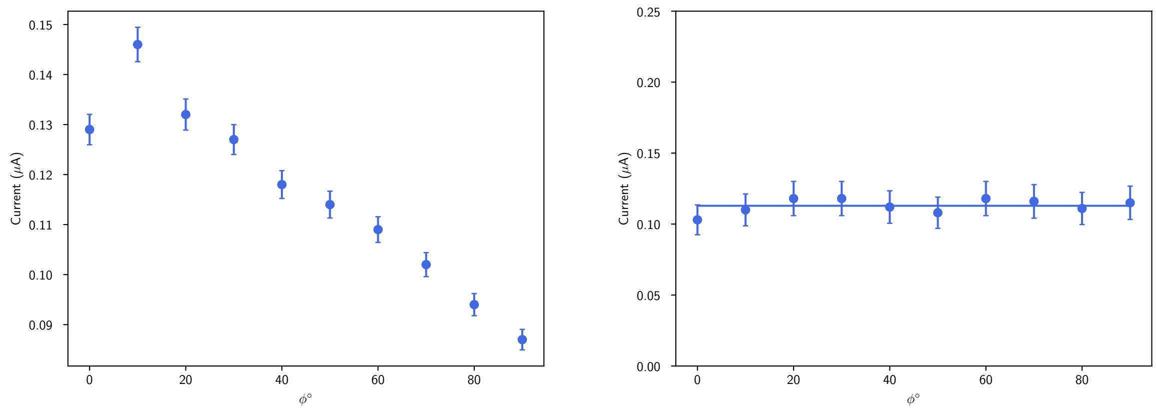

Figure 12: Graphs of intensity of scattering versus azimuthal angle from 0° to 90°. (a) Horizontal polarised light (b) Vertical polarised light.

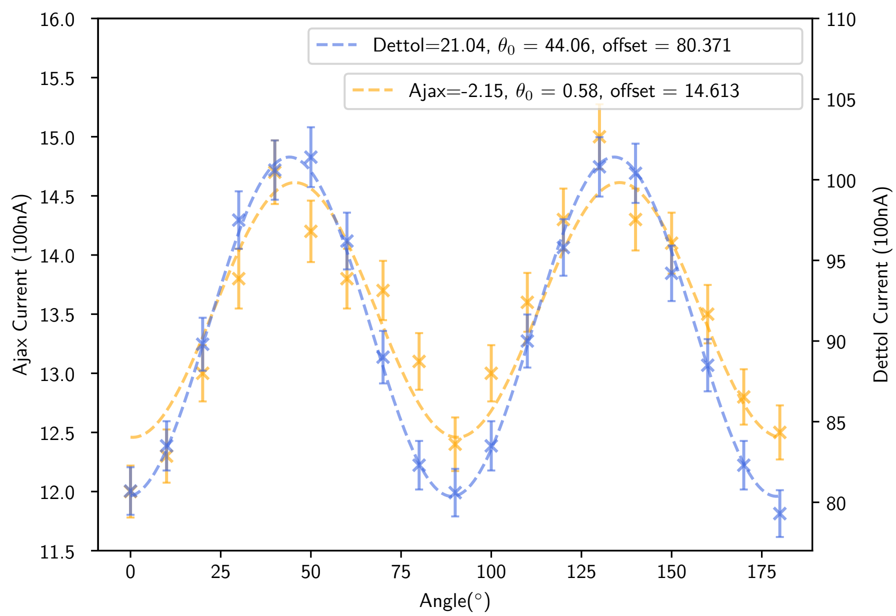

Figure 13: Curves describing intensity of scattering at a perpendicular observation angle to the beam as a function of the angle of the analyser for Ajax and Dettol superimposed on the same plot with different y axes. The important thing to note is the fact that they are in phase but with different amplitudes.

5.2.2 Polarisation

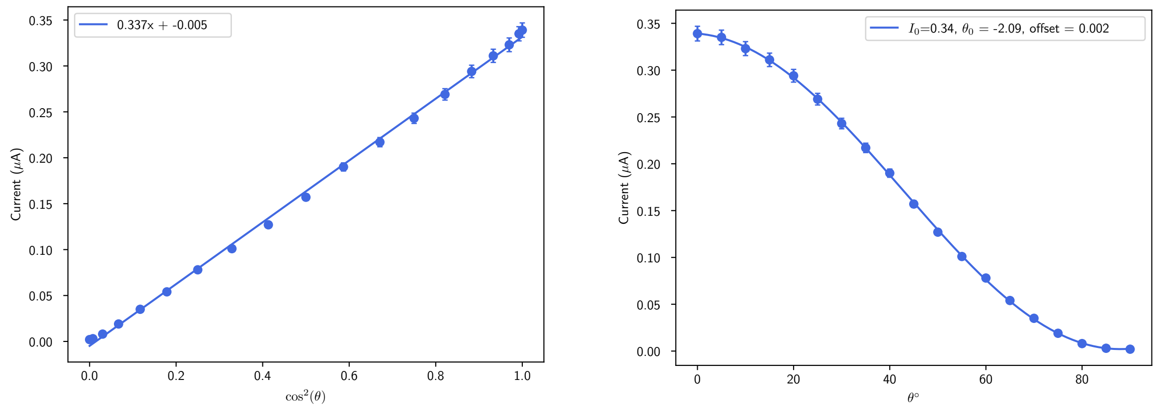

Figure 14: Results from Malus law experiment. (a) Intensity versus $\cos^2\theta$ (b) Intensity versus angle of the analyser.

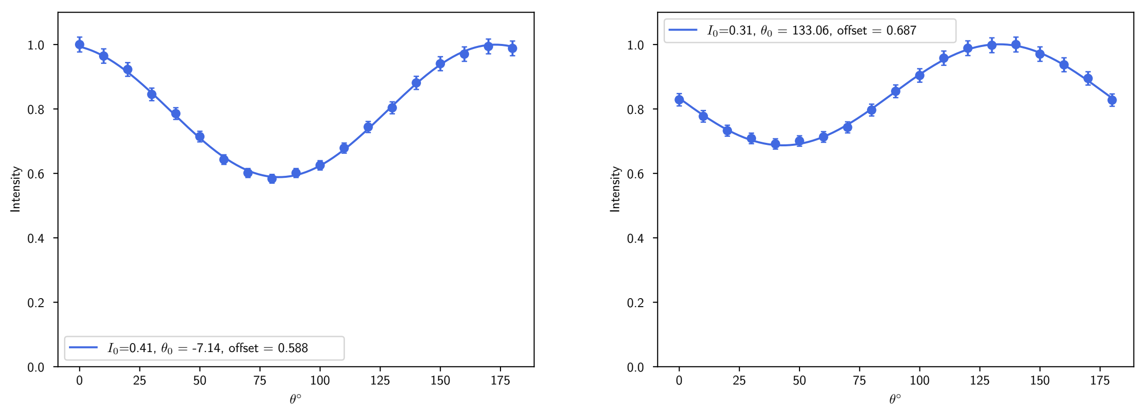

Figure 15: Similar plots to the Malus' law experiments. (a) Quarter wave plate (b) Circular polariser. Note the phase shift between the two curves.

5.3 Analysis

Our scattering results strongly reflect the theoretical model proposed in Figure 7. We found that for the intensity of scattered of light as a function of azimuthal angle, ϕ, or rotation of the spectrometer arm, it decrease monotonically from 0° to 90° in the case of horizontally polarised incident light. It seemed to decrease linearly past 20° but we currently don't have a model we can fit this to explain this relationship so we can only observe from a quasi-quantitative manner. Similarly, we found that when the incident light was vertically polarised, the intensity of the scattering along the azimuthal was largely constant, with some minor flunctuations due to deviations in background noise. Nevertheless, this agrees with our theoretical model.

We also found that the size of the molecules that scatter the photons influences the angle of scattering as postulated by Mie scattering. This is shown as the intensity of scattering at the perpendicular observation angle is much weaker for Ajax than Dettol because Dettol molecules are much bigger. However, we find that the polarisation of the scattered light is the same irregardless of molecule size as we can see the phase of the two curves are equal.

We find in Figure 14, the experimental data matches with a best fitting cosine squared function without any error.

A circular polariser is comprised of a linear polarised in front of a quarter wave plate. We find that in Figure 15(a), the coefficients of the best fitting cosine squared function is given in the legend. Comparing this with the coefficients found in Figure 15(b), we can see that the amplitudes differ by a factor of 2 but more importantly the phase difference is 215.92°. We expect the amplitude to be halved as placing a linear polariser in front of the quarter wave plate will half the effectively unpolarised light (as we don't know the orientation of this linear polariser). The phase shift is purely due to the quarter wave plate although this value heavily differs with the expected value of 90°. A better way to find the phase shift is to locate the angle of the minimums and subtract them. This method yields a result of 50.2°. However we have to consider that this is in cosine squared space where the wavelength is halved so this result will translate to a final phase delay of 100.4°, representing a 12% error.

We can verify the composition of the circular polariser but taking the ratios of each side facing the laser. We found this ratio from Side 2 to Side 1 to be $15540/0.524 \approx 30000$, i.e the side with the linear polariser must face the laser first for the light to be properly polarised before being 'twisted'.

6 Part II

6.1 Method

In the latter half of the report we want to explore the polarisation of light caused by reflecting on different materials, namely a dielectric and a metal.

6.1.1 Dielectrics

In dielectric materials such as glass, there exists a special angle, denoted as the Brewster's angle for which the reflected beam of light is maximally polarised and the angle between the reflected beam and the refracted beam is 90 degrees. We want to find this angle so we can accurately calculate the refractive index of the glass prism to then confirm Fresnel's equations.

To find Brewster's angle we replace the photodetector with a white screen and then remove the analyser attached to the spectrometer arm. The prism is then placed on the sample stage with the vertically polarised laser incident at its normal. We then rotate the polarisation of the laser until the reflected beam on the white screen hits a minimum, this happens because the incoming polarised light is now perpendicular to the plane of incidence, causing further partial polarisation of the reflected beam. Once, at the minimum, the table is incrementally rotated and the process is repeated until we achieve the absolute minimum and the angle of incidence is defined as Brewster's angle.

Since we have the refractive index, we want to verify Fresnel's equations. At the normal incidence, the associated Jones matrix to find the reflected beam is

$$\mathbf{M} = \begin{pmatrix} r & 0 \\ 0 & r \end{pmatrix}. \tag{23}$$

Derived in Appendix 7.3.2, we find that the intensity of the reflected ray divided by the intensity emitted is directly equal to the reflectance coefficient. There are many ways of obtaining this reflectance coefficient at the normal incidence. We can do a direct measurement by taking the intensity of the reflectance and dividing it by the measured intensity of the laser beam. We can also use Fresnel's equation 7 where k is 0 in this case. We will compare these values with the fitted value found experimentally.

6.1.2 Metals

Finally we want to determine the optical constants of the aluminium mirror. To do this we need to solve Equations 7 and 8 simutaneously as there are two unknowns. We can take two intensity versus analyser angle curves at different angle of incidences. Similar to experiments 2 and 3 where we just rotated the analyser through 180 degrees to obtain a Malus law curve, this time we want to produce the curves for the reflected beams for angle of incidences, 20° and 79°.

6.2 Results

6.2.1 Dielectrics

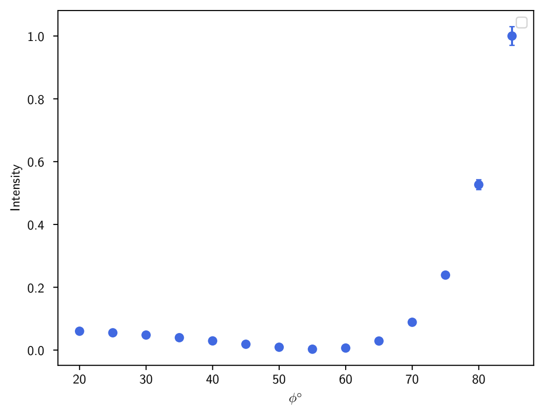

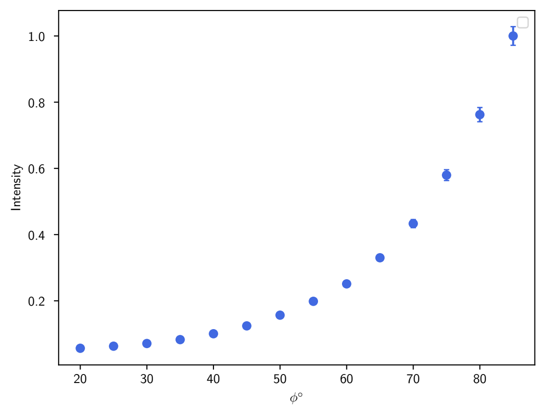

Figure 16: Minimum intensity versus azimuthal angle (a) Horizontal polarisation of incident light, resulting in R_p. (b) Vertical polarisation of incident light, resulting in R_s.

6.2.2 Metals

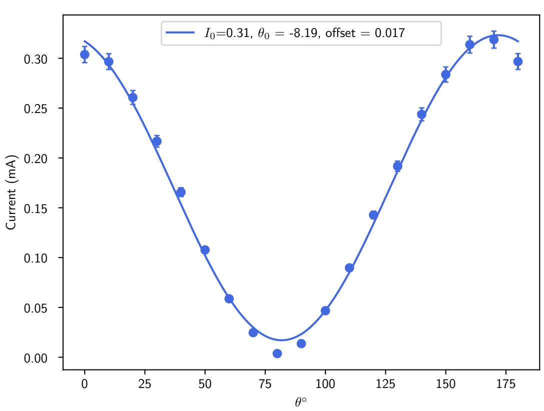

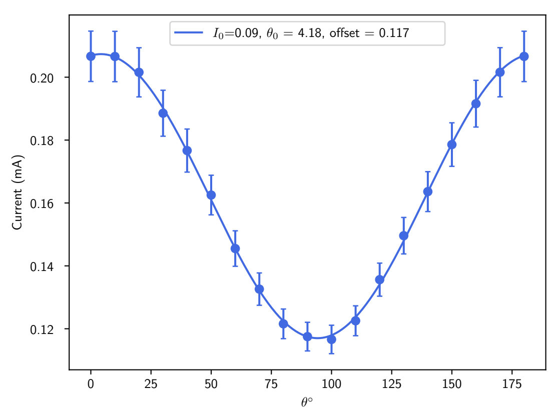

Figure 17: Intensity versus angle of analyser plot. (a) At 20° to the normal. (b) At 79° to the normal.

6.3 Analysis

We determined Brewster's angle to be $51 \pm 0.8°$. Glass is usually approximated to have a Brewster's angle of 56°, representing a 9% error. Nevertheless, this translates to a refractive index of 1.55 for our glass prism.

Using this value, we can find the reflectance coefficient using Equation 7, again where k is zero. This gives us an r value of 0.305, representing roughly 31% of light is reflected and so 69% of light is transmitted. Experimentally, we found the reflectance intensity to be $55.3nA$ whilst the laser without any reflection was found to be $339nA$, giving us a coefficient value of 0.163. This represents as a 46% deviation from the expected value given by Fresnel's equation. We can see qualitatively in Figure 16 that the experimental data deviates quite a bit away from the best fit curve whilst the error bars are quite low.

We also found that the angle of incidence on the glass prism will change the polarisation of the reflected light. Taking a measurement at 20° to the normal yielded a maximal polarisation in the direction 312° with respect to the analyser. Meanwhile, taking the same measurement but at 80°, we find that this angle has fallen to 236°. This was expected as the two angles of incidences lie on opposite sides of the Brewster angle.

Finally for the light incident on metals, we can use simutaneous equations to solve for n and k. From Figure 17, the phase difference is 12.37°. Converting this into radians, gives us 0.216. Since we didn't obtain a reflectance measurement due to negligance, we have to assume a $r = 0.65$. Solving the two equations yields us $n = 0.108$ and $k = 0.0727$

6.4 Discussion

The hardest proponent of this experiment was the alignment of the components. No matter how many tries it took to move each component around, it was difficult to align the laser directly at the detector without any reflected beams and then aligning the analyser to perfectly slide between the laser and the detector. Eventually due to the nature of the experiment exploring the relationship between quantities rather than aiming to measure a specific accurate value, perfect alignment was forgone.

The latter half of the experiment provided great challenges in utilising the prism due to its shape. It was difficult to produce great angles of incidence to the normal so we had to forgo perfect alignment in order to compensate for the prism's shape.

Another large issue was the lack proper uncertainty analysis when it comes to angles. Since the size of the angle did not matter, it was the size of the angle relative to other readings that did, it was hard to quantify this value as a percentage error.

6.5 Conclusion

These experiments were completed in a satisfactory manner. They explored various features and causations of polarisations however lacked the accuracy and precision required to draw out definitive conclusions about the relationships involved.

7 Appendix

7.1 Pre-Work Theoretical Questions

7.1.1 Question 2a

What is the condition for linearly polarised light to remain unaltered as it passes through a crystal?

For the linearly polarised light to remain unaltered, the light incidence needs to experience no relative phase changes. Crystals can either be isotropic or anisotropic. In the case of isotropic crystals, the linearly polarised light has to be pass through the crystal along its polarisation axis. Anisotropic materials have a property known as birefringence, where the crystal has a different refractive index for each polarisation and propagation of light. The linearly polarised light must enter the crystal along the optical axis. This means that the light will only experience the refractive index of ordinary rays. If light were to enter the crystal in any other direction, then it would experience two refractive indexes which will alter the polarisation of the wave. Similarly, in biaxial crystals, there are two optical axes (binormals) that allow light to travel through without birefringence.

7.1.2 Question 2b

What are the conditions to create circularly polarised light?

You can use a linear polariser to get linearly polarised light first and then use a quarter wave layer to create a circular polariser. The corresponding phase difference needs to be 90 degrees. To achieve this, the formula for phase difference in uniaxial crystals can be used,

$$\Delta\phi = \frac{2\pi}{\lambda}(n_e - n_o)d. \tag{24}$$

By adjusting the thickness, d, of the crystal appropriately as n_e and n_o are fixed, we can obtain a phase difference of 90 degrees. Then the quarter wave plate needs to placed at an angle of 45 degrees with the plane of the incident polarised light.

7.1.3 Question 2c

What is the effect of a quarter wave plate on circularly polarised light?

The quarter wave plate will introduce a 90 degree phase shift which will convert circularly polarised light back to linearly polarised.

7.1.4 Question 2d

What is the effect of a half wave plate on circularly polarised light?

A half wave plate will introduce a phase difference of 180 degrees, meaning that the handedness of the circular polarisation will switch i.e right handed circular polarisation will turn into left handed circular polarisation and vice versa.

7.1.5 Question 2e

Sometimes the scattering of light off particles may lead to polarisation. Explaining in terms of scattering, why is the sky blue and why clouds are grey?

In 1871, Rayleigh discovered that when light is scattered by molecules or particles much smaller than the wavelength of the light, the intensity of the scattered light has the following property,

$$I \propto \frac{1}{\lambda^4}. \tag{25}$$

This is why the sky is blue as the lower wavelengths of light, i.e bluer, are scattered much more. At sunset, when the sun is low of the horizon, the blue and violet light is scattered out of the direct line of sight, giving the sky its redder tinge. In clouds, the particles are no longer small enough for Rayleigh scattering and instead we look at Mie scattering. Here we find that the droplets of water will scatter all wavelengths equally and so clouds are perceived as white. As the clouds become thicker, more light is absorbed and less sunlight can penetrate, dimming the sky and the appearance of the cloud.

When light strikes a particle, it will induce an oscillation in the charges of the particle, causing it to re-emit light but they do so more strongly in directions where the electric field is perpendicular to the direction of observation. For the original incoming light, it becomes polarised as the electric field in the direction of scattering is minimised.

7.1.6 Question 2f

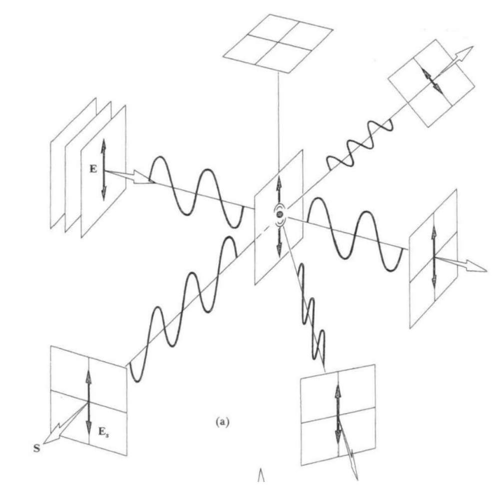

Figure 18: Scattering of polarised light by a molecule

Scattered light will only propagate in forward directions and not in the direction of the electric field. The magnitude will be equal in the directions orthogonal to the propagation of the electric field and decrease as the angle between the propagation of the scattered wave and the propagation of the original wave's electric field is smaller.

7.1.7 Question 2g

Using

$$I_1 = I_0 \cos^2 \theta. \tag{26}$$

a. 100% b. 50% c. 0%

7.2 Lab Book

7.2.1 Proper Attempt

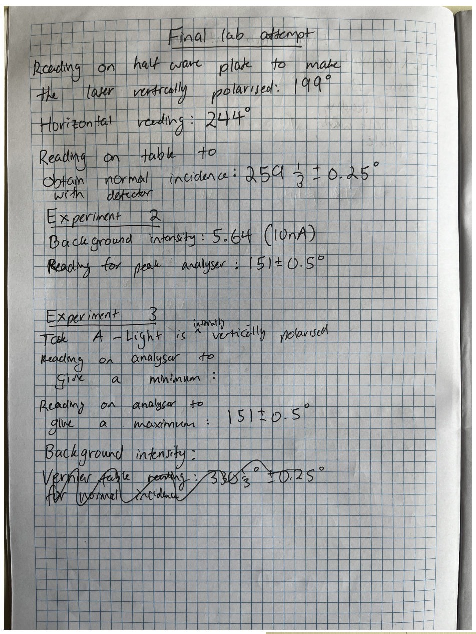

Final lab attempt

Reading on half wave plate to make the laser vertically polarised: 199°

Horizontal reading: 244°

Reading on table to obtain normal incidence with detector: $259\frac{1}{3} \pm 0.25°$

Experiment 2

Background intensity: 5.64 (10nA)

Reading for peak analyser: $151 \pm 0.5°$

Experiment 3

Task A - Light is initially vertically polarised

Reading on analyser to give a minimum:

Reading on analyser to give a maximum: $151 \pm 0.5°$

Background intensity:

~~Vernier table reading for normal incidence~~: ~~$330\frac{1}{3}°$~~ $\pm 0.25°$

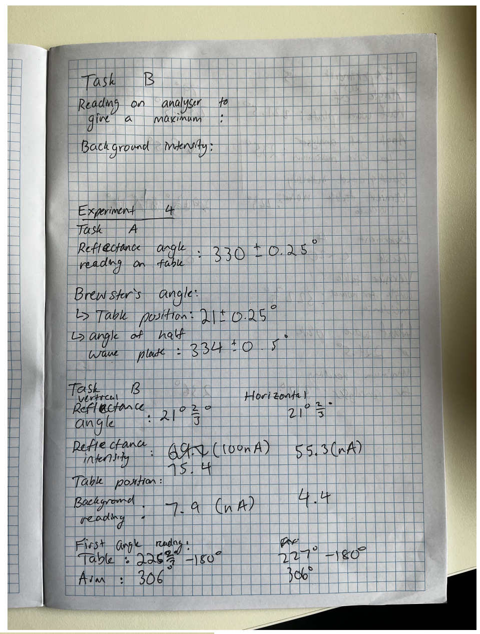

Task B

Reading on analyser to give a maximum:

Background intensity:

Experiment 4

Task A

Reflectance angle reading on table: $330 \pm 0.25°$

Brewster's angle:

↳ Table position: $21 \pm 0.25°$

↳ angle of half wave plate: $334 \pm 0.5°$

Task B

	Vertical	Horizontal
Reflectance angle	$21°\frac{2}{3}°$	$21°\frac{2}{3}°$
Reflectance intensity	~~69.2~~ (100nA) 75.4	55.3 (nA)
Table position:		
Background reading	7.9 (nA)	4.4

First angle reading:

Table: $226\frac{2}{3}°$ −180° | 227° −180°

Arm: 306° | 306°

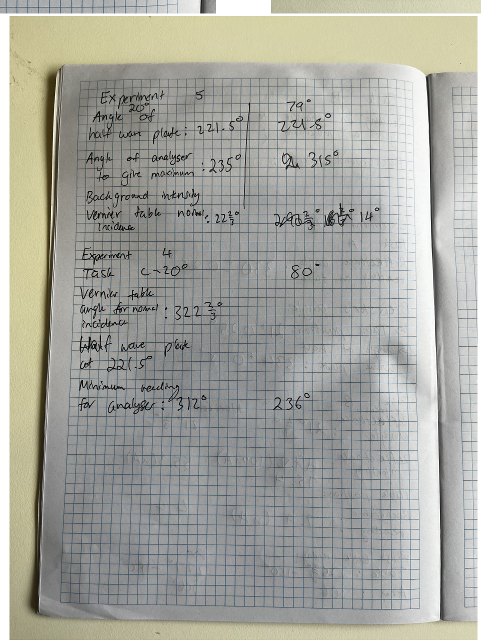

Experiment 5

	20°	79°
Angle of half wave plate:	221.5°	221.5°
Angle of analyser to give maximum:	235°	315°
Background intensity		
Vernier table normal incidence:	$22\frac{2}{3}°$	14°

Experiment 4

Task C ~20° | 80°

Vernier table angle for normal incidence: $322\frac{2}{3}°$

Half wave plate at 221.5°

Minimum reading for analyser: 312° | 236°

7.2.2 Failed Attempts

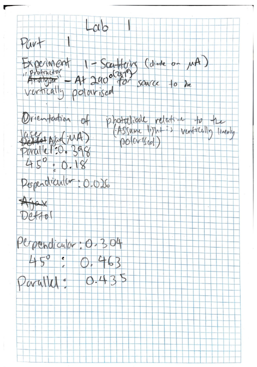
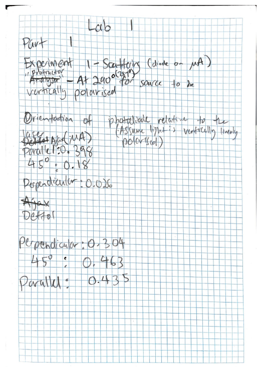
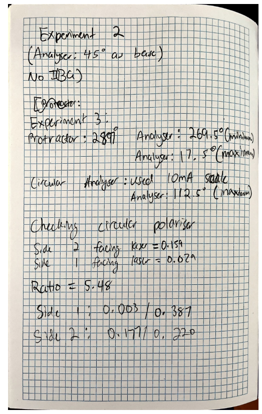
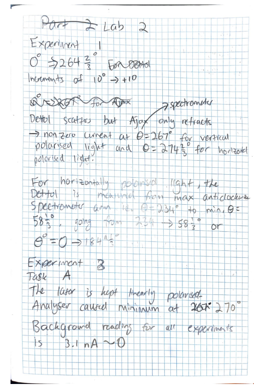
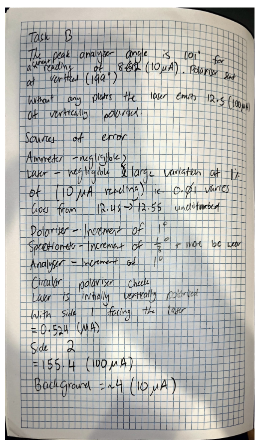
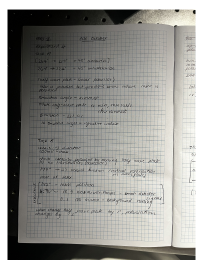
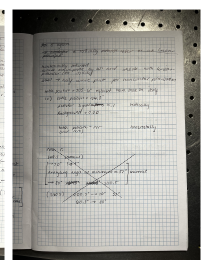

7.3 Derivations

7.3.1 Quarter wave plate using Jones matrices

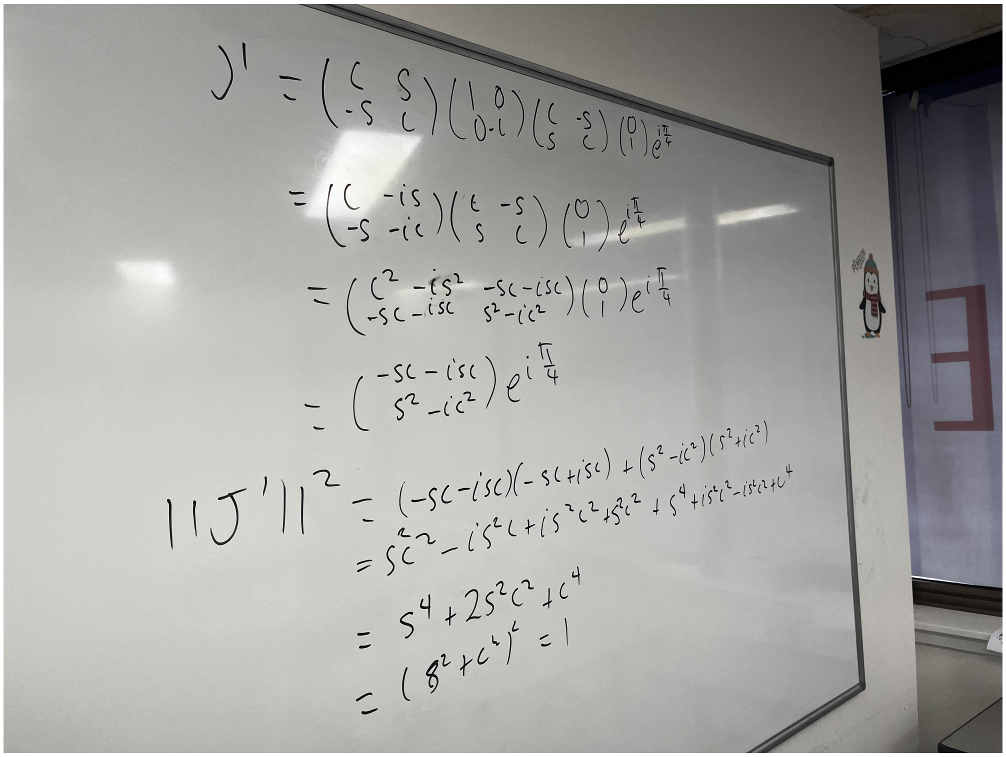

7.3.2 Reflectance coefficient using Jones matrices

$$J' = \begin{pmatrix} c & s \\ -s & c \end{pmatrix} \begin{pmatrix} r & 0 \\ 0 & r \end{pmatrix} \begin{pmatrix} c & -s \\ s & c \end{pmatrix} \begin{pmatrix} 0 \\ 1 \end{pmatrix}$$

$$= \begin{pmatrix} cr & sr \\ -sr & cr \end{pmatrix} \begin{pmatrix} c & -s \\ s & c \end{pmatrix} \begin{pmatrix} 0 \\ 1 \end{pmatrix}$$

$$= \begin{pmatrix} c^2 r + s^2 r & -scr + scr \\ -scr + scr & s^2 r + c^2 r \end{pmatrix} \begin{pmatrix} 0 \\ 1 \end{pmatrix}$$

$$= \begin{pmatrix} r & 0 \\ 0 & r \end{pmatrix} \begin{pmatrix} 0 \\ 1 \end{pmatrix}$$

$$= \begin{pmatrix} 0 & 0 \\ 0 & r \end{pmatrix}$$

$$|J|^2 = r^2$$

7.4 Curve fitting

Python was used to create theoretical models to best fit the experimental data. First the cosine squared function was defined with parameters: I_0, theta0 and offset with variable theta. The amplitude is given by the initial intensity, I_0, the phase shift is given by theta0 and the vertical displacement of the funtion is given by the parameter offset.

```
def curve(theta,I_0,theta0,offset):
    return I_0 * np.cos(np.radians((theta - theta0)))**2 + offset
```

Using the scipy optimize package, the curve fit function can be used which uses a least-squares algorithm to guess the parameters that best fits the data input. An example can be seen below,

```
x = data['Angle (degrees)']
y = data['Current (micro amps)']

param,covariance = sp.curve_fit(curve,x,y)
```

The return of the function is of course an array, param, of the best fitting parameters.

Rather than plotting the model as a function of the experimental data, the model was plotted over a a higher resolution of x values to provide a smoother curve.

```
x_smooth = np.linspace(x.min(),x.max(),1000)
y_smooth = curve(x_smooth,*param)
plt.plot(
    x_smooth,
    y_smooth,
    label=rf'$I_0$={param[0]:.2f}, $\theta_0$ = {param[1]:.2f}, offset = {param[2]:.3f}'
)
```

The Fresnel equations were also fitted using the following code.

```
def fresnel_s(theta, E_p, I_0, n=1.5, epsilon=1e-4):
    theta_rad = np.radians(theta)

    small_angle_mask = np.abs(theta_rad) < epsilon
    large_angle_mask = ~small_angle_mask

    result = np.zeros_like(theta_rad)

    result[small_angle_mask] = I_0 + E_p * (theta_rad[small_angle_mask] ** 2) / 2

    refracted_theta = np.arcsin(np.sin(theta_rad[large_angle_mask]) / n)
    result[large_angle_mask] = (
        E_p * np.tan(theta_rad[large_angle_mask] - refracted_theta) /
        np.tan(theta_rad[large_angle_mask] + refracted_theta) + I_0
    )

    return result

def fresnel_p(theta, E_p, I_0, n=1.5, epsilon=1e-4):
    theta_rad = np.radians(theta)

    small_angle_mask = np.abs(theta_rad) < epsilon
    large_angle_mask = ~small_angle_mask

    result = np.zeros_like(theta_rad)

    result[small_angle_mask] = I_0 + E_p * (theta_rad[small_angle_mask] ** 2) / 2

    refracted_theta = np.arcsin(np.sin(theta_rad[large_angle_mask]) / n)
    result[large_angle_mask] = (
```

```
        E_p * np.tan(theta_rad[large_angle_mask] - refracted_theta) /
        np.tan(theta_rad[large_angle_mask] + refracted_theta) + I_0
    )

    return result
```

7.5 Solving simutaneous equations

```
# Define the functions for fsolve
def equations(vars):
    x, y = vars
    eq1 = np.arctan(2 * x / (1 - x**2 - y**2)) - 0.216
    eq2 = ((1 - x)**2 + y**2) / ((1 + x)**2 + y**2) - 0.65
    return [eq1, eq2]

# Provide an initial guess for (x, y)
initial_guess = (0.5, 0.5)
solution = fsolve(equations, initial_guess)
print(solution)
```